The Libyan Journal of Science (An International Journal): Volume 24, 2021

Use of Finite Difference Time Domain (FDTD) Technique to Calculate Poynting Vector in Free Space with Obstacles in Computational Domain

Sedig S. Farhat
University of Tripoli, Faculty of Science, Physics Department
Email: sedigfarhat@yahoo.co.uk

Abstract

In this paper, electromagnetic simulations in the two- and three-dimensions systems are performed by the finite difference time domain (FDTD) technique. The method can be applied for solving Maxwell's curl equations numerically to calculate the Poynting vector distributions when placing the obstacles in the centre of a domain. Perfect electric conductor (PEC) structures of convenient shapes were constructed based on the geometric shape of the obstacle such as two parallel strips and triangle shapes in order to make a comparison between the simulations. The FDTD method will determine the values of the electric and magnetic field at any point in space and the grid is terminated with the first-order Gerrit Mur's absorbing boundary condition (ABC) [1]. The boundary condition can be included in the calculations to absorb the waves when striking the boundaries. The ABC can affect the accuracy of the solutions as the calculations results demonstrate that good numerical performance of the FDTD obtained when utilizing the Mur's ABC. In the provided examples, the achieved results indicate that very good radiation patterns were obtained when ABCs are implemented at all the edges. The results of FDTD simulations have shown that we have simulated the wave propagation in open domains.

Key words: Maxwell's curl equations; finite difference time domain (FDTD) method; Mur's first-order absorbing boundary condition (ABC); three-dimensions (3-D); two dimensions (2-D), transverse magnetic mode (TM_z mode).

المستخلص

تم في هذه الورقة محاكاة الموجات الكهرومغناطيسية باستخدام طريقة الفروق المحددة لحل معادلات ماكسويل مع تطبيق شروط الحدية موروتوليد الموجات فى الفضاء المحتوي على عوائق من موصل مثالي مثل شريطين متوازيين وشكل مثلث. تم حساب متجه بوينتك والحصول على نتائج فى بعدين وايضا فى ثلاثة ابعاد. وتبين من النتائج عند تطبيق شرط الحد مور محاكاة فضاء لانهائى.

Accepted for Publication: 20/6/2021

Introduction

Electromagnetic wave propagations will be numerically studied when including an obstacle in a computational domain and this is not easily described analytically. To overcome this difficulty, there are many different numerical techniques employed to calculate the fields such as the FDTD method. It is well known that this method employes solving Maxwell's curl equations numerically by utilizing the central difference approximation. This method has been applied to solve many kinds of problems such as in medical application, and in predication of electromagnetic wave propagation, in studying plasma [2] and in communication system [3]. In this paper, we consider the propagations of electromagnetic waves in free space without and with including an obstacle in a domain as well as consider the behaviour of electromagnetic waves without and with an absorbing boundary condition. The FDTD simulation is studying the behaviour of EM wave in time in response to to a source exciting the domain. We have studied the distributions of Poynting vector when interacting of electromagnetic wave with an obstacle. We constructed the obstacles with different shapes located at the centre of a domain and the distance between the obstacle and the boundary filled with air. The obstacles will diffract and scatter the wave which can cause to vary the distributions of the fields. Therefore, the aim of this work is to describe how 2-D FDTD and 3-D FDTD approaches is utilized to study electromagnetic wave propagation in space containing a perfect electric conductor (PEC). Electromagnetic waves will impact with a perfect electric conductor obstacle as the distributions of the scattered fields will vary when including different shapes and size. The PEC structures of convenient shapes have been chosen by mapping each shapes into the domain to make a comparison in term of their distributions between the simulations. Once the electromagnetic field components are determined at every time step in each cell then Poynting vector can be calculated in each pixel and voxel at every time step in two and three dimensions, respectively. There are many shapes which could generate different distributions. Therefore, many examples can be studied such as a triangle geometric shape included in a domain. This is a very complicated structure to construct in a space. It can be done by generating the obstacles as a mesh mode in a domain. Moreover, the ABCs must be used in the FDTD simulation, because the computer's storage and more memory are limited. Therefore, a computational domain must be utilized with limited size [4]. This problem can be solved by employing a method like absorbing boundary condition (ABC) to terminate a FDTD grid. It is well known that the space is required to be truncated to simulate an open space to prevent the reflections coming from the edges. To overcome this problem, it is therefore important to have the ABC in a computational domain to allow the waves to propagate into the infinite space without reflecting back. Because, the reflections will cause the waves to interfere with each other in the computational domain and this will produce reflection patterns. This will affect the numerical accuracy of the calculations. Therefore, part of this work was carried out to demonstrate how to implement the ABC and why an absorbing boundary condition should be included in a computational domain during the calculations which is very important to improve the accuracy of the calculations. It is also significant

to know that one of main advantage of the ABC is reducing computational time by decreasing the size of computational domain as the calculation will not include unnecessary large size storage arrays. This will lead to improve the FDTD performance and then obtain an accurate field distribution. Therefore, the boundaries will be implemented on all faces by applying the Mur's approach [1]. This study will investigate the impact of including an obstacles in the space and the interactions of EM wave with obstacles which will be observed when the problem space is simulated as if it is surrounded by an open domain. Therefore, an example illustrating the effect of the implementation of the absorbing boundary conditions will be provided by computing the distributions of all components and the numerical calculations of interaction of the emitted EM wave with obstacles will be demonstrated in the results section.

Method

We can briefly describe the basic of the finite difference time domain (FDTD) method which was first proposed by Kane Yee [5] in 1966. The technique is a numerical method based on a finite difference concept that can be applied to find a solution of time dependent Maxwell's curl equations:

$$\frac{\partial \mathbf{E}}{\partial t} = \frac{1}{\varepsilon_o} \nabla \times \mathbf{H} \tag{1.a}$$

$$\frac{\partial \mathbf{H}}{\partial t} = -\frac{1}{\mu_o} \nabla \times \mathbf{E} \tag{1.b}$$

Where the **E** is the electric field and **H** is magnetic field.

The central finite difference approximation method applied to generate six discrete update equations to simulate a system in three dimensions case. Therefore, the field components can be written as the first in three dimensions case and second in two dimensions case since this study in this work is divided into two parts. The following equations can be utilized to update the electric field components in three-dimensional simulations [5, 6]:

$$E_x\big|_{i+\frac{1}{2},j,k}^{n+1} = E_x\big|_{i+1/2,j,k}^{n} + \frac{1}{\varepsilon_o}.\left(\frac{\Delta t}{\delta}\left(H_z\big|_{i+\frac{1}{2},j+\frac{1}{2},k}^{n+\frac{1}{2}} - H_z\big|_{i+\frac{1}{2},j-\frac{1}{2},k}^{n+\frac{1}{2}}\right) - \frac{\Delta t}{\delta}\left(H_y\big|_{i+\frac{1}{2},j,k+\frac{1}{2}}^{n+\frac{1}{2}} - H_y\big|_{i+\frac{1}{2},j,k-\frac{1}{2}}^{n+\frac{1}{2}}\right)\right) \tag{2.a}$$

$$E_y\big|_{i,j+\frac{1}{2},k}^{n+1} = E_y\big|_{i,j+1/2,k}^{n} + \frac{1}{\varepsilon_o}.\left(\frac{\Delta t}{\delta}\left(H_x\big|_{i,j+\frac{1}{2},k+\frac{1}{2}}^{n+\frac{1}{2}} - H_x\big|_{i,j+\frac{1}{2},k-\frac{1}{2}}^{n+\frac{1}{2}}\right) - \frac{\Delta t}{\delta}\left(H_z\big|_{i+\frac{1}{2},j+\frac{1}{2},k}^{n+\frac{1}{2}} - H_z\big|_{i-\frac{1}{2},j+\frac{1}{2},k}^{n+\frac{1}{2}}\right)\right) \tag{2.b}$$

$$E_z\big|_{i,j,k+\frac{1}{2}}^{n+1} = E_z\big|_{i,j,k+1/2}^{n} + \frac{1}{\varepsilon_o}.\left(\frac{\Delta t}{\delta}\left(H_y\big|_{i+\frac{1}{2},j,k+\frac{1}{2}}^{n+\frac{1}{2}} - H_y\big|_{i-\frac{1}{2},j,k+\frac{1}{2}}^{n+\frac{1}{2}}\right) - \frac{\Delta t}{\delta}\left(H_x\big|_{i,j+\frac{1}{2},k+\frac{1}{2}}^{n+\frac{1}{2}} - H_x\big|_{i,j-\frac{1}{2},k+\frac{1}{2}}^{n+\frac{1}{2}}\right)\right) \tag{2.c}$$

And use of the following equations to update the magnetic fields components:

$$H_x|_{i,j+1/2,k+1/2}^{n+1/2} = H_x|_{i,j+1/2,k+1/2}^{n-1/2} + \frac{1}{\mu_o}.\left(\frac{\Delta t}{\delta}\left(E_z|_{i,j,k+1/2}^{n} - E_z|_{i,j+1,k+1/2}^{n}\right) - \frac{\Delta t}{\delta}\left(E_y|_{i,j+1/2,k}^{n} - E_y|_{i,j+1/2,k+1}^{n}\right)\right) \quad (2.d)$$

$$H_y|_{i+1/2,j,k+1/2}^{n+1/2} = H_y|_{i+1/2,j,k+1/2}^{n-1/2} + \frac{1}{\mu_o}.\left(\frac{\Delta t}{\delta}\left(E_z|_{i+1,j,k+1/2}^{n} - E_z|_{i,j,k+1/2}^{n}\right) - \frac{\Delta t}{\delta}\left(E_x|_{i+\frac{1}{2},j,k+1}^{n} - E_x|_{i+1/2,j,k}^{n}\right)\right) \quad (2.e)$$

$$H_z|_{i+1/2,j+1/2,k}^{n+1/2} = H_z|_{i+1/2,j+1/2,k}^{n-1/2} + \frac{1}{\mu_o}.\left(\frac{\Delta t}{\delta}\left(E_x|_{i+1/2,j+1,k}^{n} - E_x|_{i+1/2,j,k}^{n}\right) - \frac{\Delta t}{\delta}\left(E_y|_{i+1,j+1/2,k}^{n} - E_y|_{i,j+1/2,k}^{n}\right)\right) \quad (2.f)$$

With regard to the two-dimensional simulations, we will utilize the transverse magnetic (TM_z) mode and the discrete update equations can be given as [5]:

$$H_x^{n+\frac{1}{2}}(i, j+\tfrac{1}{2}) = H_x^{n-\frac{1}{2}}(i, j+\tfrac{1}{2}) - \frac{\delta t}{\mu_0\,\delta}\left(E_z^n(i, j+1) - E_z^n(i, j)\right) \quad (3.a)$$

$$H_y^{n+\frac{1}{2}}\left(i+\tfrac{1}{2}, j\right) = H_y^{n-\frac{1}{2}}\left(i+\tfrac{1}{2}, j\right) + \frac{\delta t}{\mu_0\,\delta}\left(E_z^n(i+1, j) - E_z^n(i, j)\right) \quad (3.b)$$

$$E_z|_{i,j}^{n+1} = E_z|_{i,j}^{n} + \frac{1}{\varepsilon_o}.\left(\frac{\Delta t}{\delta}\left(H_y|_{i+\frac{1}{2},j}^{n+\frac{1}{2}} - H_y|_{i-\frac{1}{2},j}^{n+\frac{1}{2}}\right) - \frac{\Delta t}{\delta}\left(H_x|_{i,j++\frac{1}{2}}^{n+\frac{1}{2}} - H_x|_{i,j-\frac{1}{2}}^{n+\frac{1}{2}}\right)\right) \quad (3.c)$$

The FDTD updating equations provided in equations (2) and equations (3) will be applied to solve three- and two-dimensions cases, respectively. These equations can be implemented in the computer programs to calculate the electric and magnetic field components at each time step in a computational domain with including the obstacles at the centre of a domain. The calculated field components will be used to compute the Poynting vector that given by:

$$\mathbf{S} = \mathbf{E} \times \mathbf{H} \quad (4)$$

The cross product of the **E** with **H** will provide the direction of propagation of the EM wave in space. Therefore, the Poynting vector (Watt/m^2) can be computed in each pixel in 2-D case and each voxel in 3-D case.

Furthermore, the first-order Mur's absorbing boundary condition will be applied and the FDTD updating equation at the boundary as an example in 3-D case at *x*=0 gird boundary [1] given by:

$$E_z^{n+1}(0, j, k+1/2) = E_z^n(1, j, k+1/2) + \frac{(c\delta t - \delta)}{(c\delta t + \delta)}\left(E_z^{n+1}(1, j, k+1/2) - E_z^n(0, j, k+1/2)\right) \quad (5)$$

Similar equations will be implemented for other electric field components in mesh walls in 3-D and 2-D simulations which can be applied to absorb the reflections generated from the six boundaries in 3-D FDTD simulations and four boundaries in 2-D FDTD simulations. Therefore, the performance of Mur ABC will be demonstrated in the result section.

Results and Discussion

The FDTD calculations were performed, the results of simulations were demonstrated and the output of the programs was wrote by a computer MATLAB (R2013a) programming language. The FDTD simulations were written based on equations (2) and equations (3) for computing the field components in 3-D FDTD and 2-D FDTD, respectively. These components will be utilized to calculate the Poynting vector based on equation (4) as a pixel by pixel in two-dimensional in the *x-y* plane whereas a voxel by voxel in three-dimensional in the *x*, *y* and *z* directions. The size of each cell was chosen as a uniform mesh in two and in three directions based on ten grid cells per wavelength which is required for accuracy and the time step must satisfy the Courant condition in order for the solution to be stable, which is provided by [1, 2]:

$$\Delta t \leq \frac{\delta}{c\,(n)^{1/2}} \qquad (6)$$

Where the δ is the space increment, c is the speed of light in space and *n* is the dimensionality of the problem such as *n*=2, 3 for simulating a two-dimensional and three-dimensional systems, respectively.

The FDTD simulation will consider the behaviour of electric and magnetic fields every time step due to exciting a domain and can study the effect of the boundary condition on the calculations by comparing the results of the simulations when including the ABC to obtain an accurate result and the simulation without including ABC. The latter will affect the calculation and the accuracy of the calculations as the EM wave when reaching the end of a domain, the wave reflects back in space. Therefore, we have studied the propagation behaviour of the TM_z wave without ABC and with Mur's ABC. The purpose of the numerical example is to demonstrate the performance of the Mur's ABC. The numerical results of the TM_z mode showed that the source of excitation generated the wave and spread on the *x-y* plane by using a sinusoidal wave with frequency 2 GHz propagating in the *x-y* plane in 2-D and all snapshots are taken at 500 time steps. From figure 1 can demonstrate that how the TM_z wave propagate in free space and once the waves reaching the boundary, the waves will hit the walls and then reflecting back to the domain and propagating everywhere in the problem space then producing the reflection patterns. It can be clearly seen that there are significant differences in the distributions between the simulations as well as the simulation without the ABCs affected a uniformity of the distribution of the Poynting vector. The reflection patterns appeared in the space as shown in figure 1. This pattern can be removed by applying the Mur's absorbing boundary condition, figure 2 shows the performance of the ABC when applying the equation 5 which found to be worked perfectly as generated the circular patterns and the grid appeared to extend into infinite. It can be said that we simulated an open domain and the example is applied to validate the implementation of the ABC and the numerical calculations have illustrated that the circular patterns produced when the wave spreading out from the source even though the waves reached at all edges, because waves absorbed by the ABCs. The boundary condition is very significant in the calculations in the FDTD and we used the Mur's absorbing boundary condition in three-dimension case as well to

reduce any reflections come from boundary to obtain good and an accurate distribution. Therefore, the results obtained in three dimensions case will demonstrate the circular patterns that can be observed in the calculations as demonstrated below *i.e*., the signals are absorbed by the boundary condition when reached at all boundaries. Moreover, we can simulate a computational domain with the obstacle included in a space. There are many type of obstacles can be included in the computational domain in term of the shapes. We can use of perfect electric conductor (PEC) obstacles which have inserted in the domain as different shapes such as small square, circular, two parallel strips and triangle as shown in figure 3 (A, B, C and D). The domain in 2-D FDTD is discretized into 100×100 cells in each example. We demonstrated the effect of a PEC obstacle on the distributions as the EM waves interact with a PEC obstacle by scattering, reflection and diffraction. The diffraction case can be achieved when an obstacle or an aperture of shape is located between the source of an excitation and point of observation *i.e.*, the diffraction will generate when the waves come cross a single slit, double slit or an obstacle in a space. This will cause the waves bend around the obstacles or during an aperture. The diffraction will allow the wave to transmit its energy around obstacles. Therefore, the purpose to include the obstacle in each calculation is that to observe the distribution of the Poynting vector when placing different shape in 2-D as well as in 3-D model. Therefore, we have made of two similar simulations in 2-D, the first case is the simulation without an obstacle as shown in figure 4 compare with the second case which is the simulation with including an obstacle such as a small square as shown in figure 5. It was noted that the distributions of the Poynting vector components affected when the waves reached the small square, the waves are scattered by the obstacle. This simulation should be compared with example when increased the size of the obstacle as illustrated in figure 6. It can be noted that the solution of the field reached the sinusoidal steady state response as the wave updated behind the structure and small values appeared in each pixel and this is known as the diffraction when the waves passing around an obstacle or during a hole while the phenomenon of reflection occurs when the wave propagating from a one medium boundary to second medium boundary, but in this study we have a PEC boundary as a second medium which will cause to generate total reflections as there is no penetrations will be seen inside an obstacle. This means that there is no transmission wave travelling into a second medium. This is due to the fact that the electric field components set to be equal zeros at regions of the obstacles. The interference patterns can be produced when an incident waves hitting an obstacle and then the waves were reflected back in space as shown in figure 5 and figure 6. Moreover, the example is given in figure 3 (C) was simulated by constructed the two parallel strips made of the PEC opened from both sides and inserted in the middle of a problem space. The domain can be excited by a point source placed at the left side of the structure.

From figure 6, there is a shadow area is clearly appeared behind the obstacle, this can be observed when increase the size of the obstacle, it can be seen that more reflection occurred on the front of the obstacle as the incident wave propagated in a domain until hitting the obstacle and then reflected to a problem space. It can be seen that the EM waves diffracted when propagating within a domain included obstacle and bending

around PEC obstacle as the wave updated in each pixel behind the obstacles, it is possible to obtain the signals behind the obstacle by recording the signals during a simulation as shown in figure 7 (A and B) which is demonstrated that the simulations reached a steady state to ensure accurate results and by increasing the size of the obstacle, the amplitude of the signal decreased. Figure 8 shows that one of the main results of the interaction of electromagnetic waves with obstacles, the diffraction can be seen and the example has shown that the waves excited in a problem space and propagated between two strips until reached the end of the structure after that start spreading out of the slit. This arrangement is demonstrated that the wave will bend when it reaches the strips on the left side of the structure and then the wave propagated within strips as well as steady state behaviour is reached. This result means that the structure appeared as a new source to transmit the signal from the left side to right side within the strips and this is due the use of two parallel strips have properties of PECs. Moreover, in the next example the source was inserted between two parallel strips, it can be noted that the components of Poynting vector appeared identical, this means that the waves are propagating bilaterally between the strips. This means that the same energy transmitted on the left side is generated on right side and the distribution appeared as spherical waves as shown in figure 9. By comparing figure 8 with figure 9, it can be seen that different distributions generated in the image, this is due changing the location of the excitation source. In the first case the source placed outside the structure while second case the source placed between the two parallel strips. Furthermore, it can be made a comparison between the simulations results when placing different obstacle shape in space as the example the Poynting vector was affected when placed a triangle in the space. It can be noted that the signals propagated everywhere in a space and when reached the obstacle split to propagate into the upper and lower regions of the obstacle and generated the same patterns and the similar wave produced as shown in figure 10. Furthermore, when we placed in a domain such as a triangle as shown in figs 11 and 12, the Poynting vectors distributions are slightly different when making a comparison with simulations results that are shown in figure 11 and figure 12. The only difference is that the obstacle in figure 11 caused more scattering in lower regions compared with obstacle in figure 12 which is caused more scattering in the upper region. Therefore, by comparing when flipping the obstacle structure, the EM field's patterns varied. Moreover, the simulation results indicate that it seems that combine figs 11 and 12 to generate the similar result that produced in figure 10. This means that the incident waves affected in the upper and lower regions in space. Therefore, it can be observed that the intensities of Poynting vector appeared identical when comparing the lower region with upper region from the middle of a domain in both simulations but when increasing the size of obstacle the interference patterns can be clearly observed and the interference patterns appeared as the incident wave excited by a source in a problem space and the wave propagate until hitting the obstacle then reflected back to the domain and then two waves added together in the same medium. The interference can be constructive or destructive and the interference will cause to vary the intensities of each component. Furthermore, we have done the similar calculations in 3-D FDTD, the domain is discretized into $100 \times 100 \times 100$ uniform cells in the x, y and z directions after that a

triangle shape placed in centre of the space in three dimensions as shown in figure 13 (A). Figure 14 shows the example of the images produced in the 3-D FDTD and the snapshots are taken at 250 time steps and circular radiation patterns appeared in the results. This can be indicated that the first order Mur's absorbing boundary condition (ABC) is an efficient to apply to absorb the EM field at boundaries in three dimensions problem. Figure 15 is displayed the field components and can be noted that there are no the electric or magnetic fields produced in the obstacle, this is due to the fact that the obstacle has property of the perfect electric conductors (PECs).Therefore, two different obstacles shapes included in the FDTD domain as shown in figure 13 (A and B). This will vary the distributions of the fields in the domain as can be clearly seen that there are two distributions generated in the space as can be seen in figure 14 and 15. The difference in the numerical results between figs 14 with 15 can be observed as more signals generated behind the second case as shown in figure 15 and the lower part is cut from the middle of the structure and there is no PEC which it is filled by a free space. It can be compared the results of simulations of the 2D FDTD with 3-D simulations when placed the triangle shape as shown in figure 10 and figure 14. It can be noted that high amplitude of signals generated between the obstacles and the source of excitation compared with behind the obstacles and also the shadow regions clearly appeared in the images in two simulations as there are less signals generated in this area. This is because there are no signals propagated inside the obstacles. Moreover, the example for two parallel strips in three-dimensional when including in a domain as shown in figure 16 and exciting the problem space by a source located between the two strips. The result of the simulation showed that the wave is propagating bilaterally. This achieved simulation result is a quite similar to the one observed in 2-D FDTD simulation as have demonstrated in figure 9.

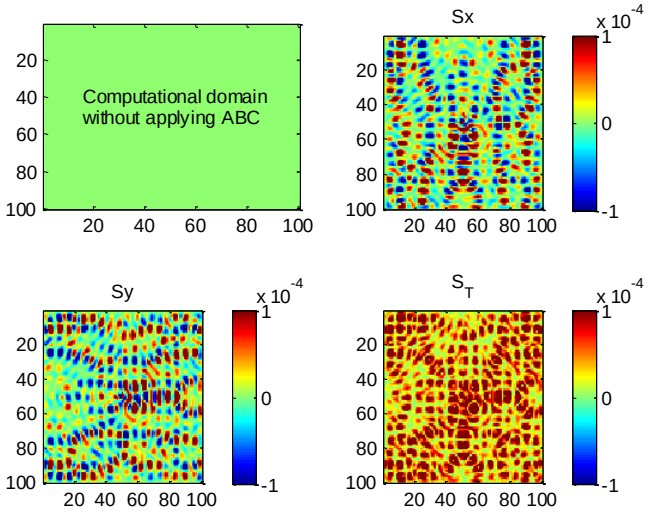

Figure 1. Snapshots of Poynting vector (Watt/m^2) taken at 500-time steps, without including an absorbing boundary condition (ABC) in the computational domain in 2-D FDTD domain.

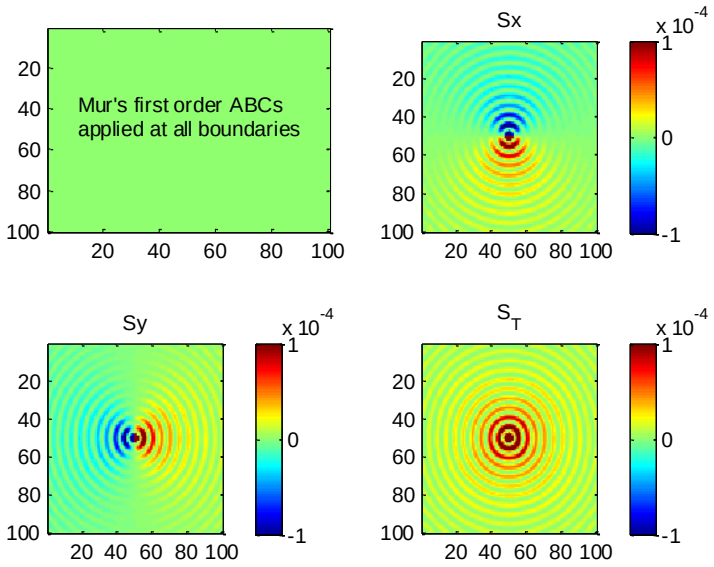

Figure 2. Snapshots taken at 500 time steps and the computational domain is terminated by the first-order Mur's ABCs in 2-D FDTD domain.

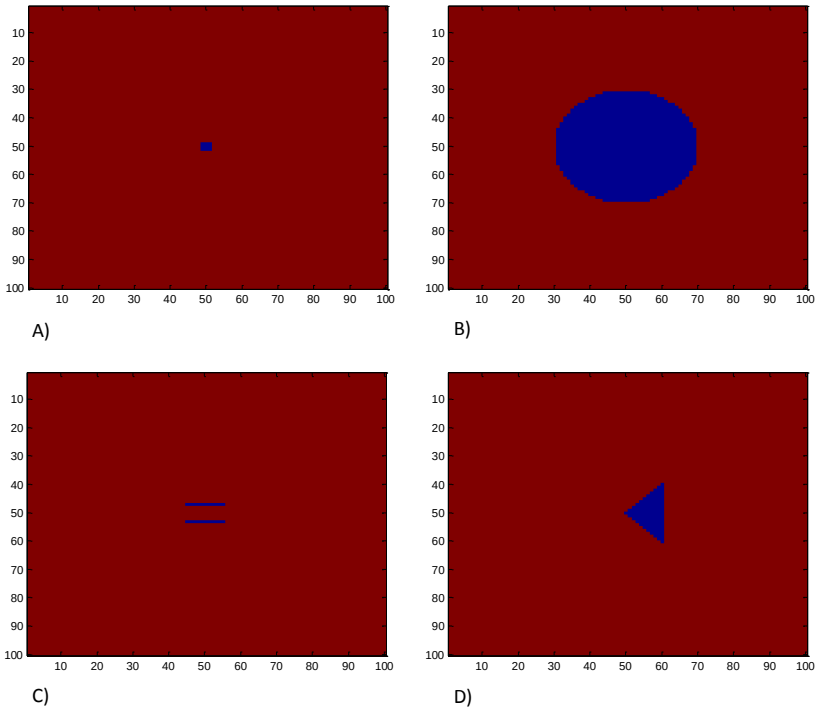

Figure 3. Two-dimensional: Four different obstacles are located in the centre of the domain and the obstacles have property of the perfect electric conductor (PEC). The FDTD cell is equal to a one-tenth of the wavelength of interest.

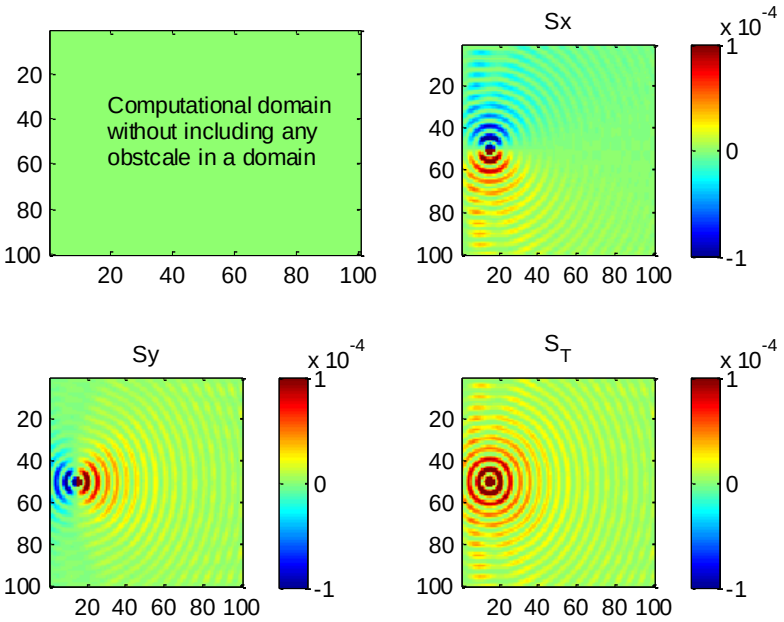

Figure 4. The source of excitation is placed on the left side of a domain without including an obstacle in space in 2-D FDTD domain.

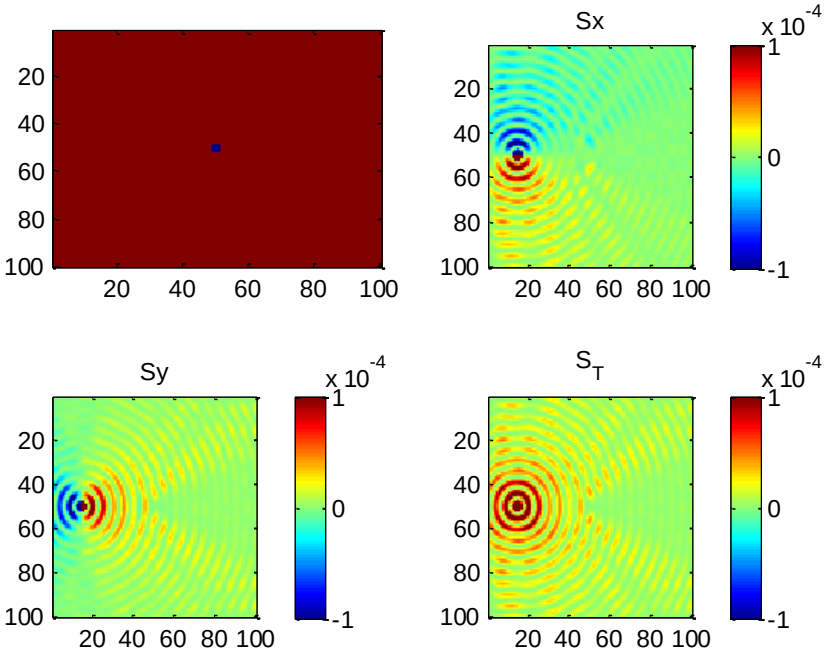

Figure 5. An obstacle as a square shape is located at the centre of a domain in 2-D FDTD.

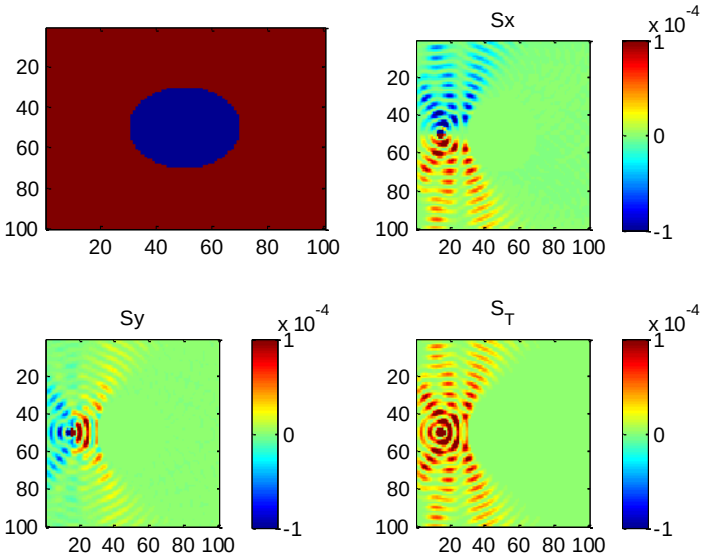

Figure 6. An obstacle as a circular shape is placed at the centre of a domain in 2-D FDTD.

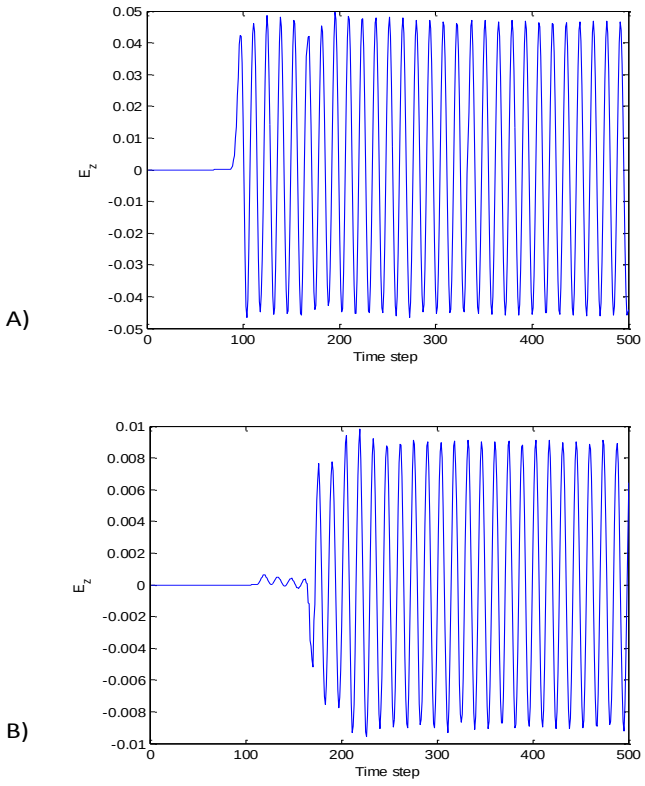

Figure 7. Signals were recorded behind the obstacles, exactly between the obstacle and the right side of the computational domain: A) the first case behind the square obstacle and B) second case behind the circular obstacle.

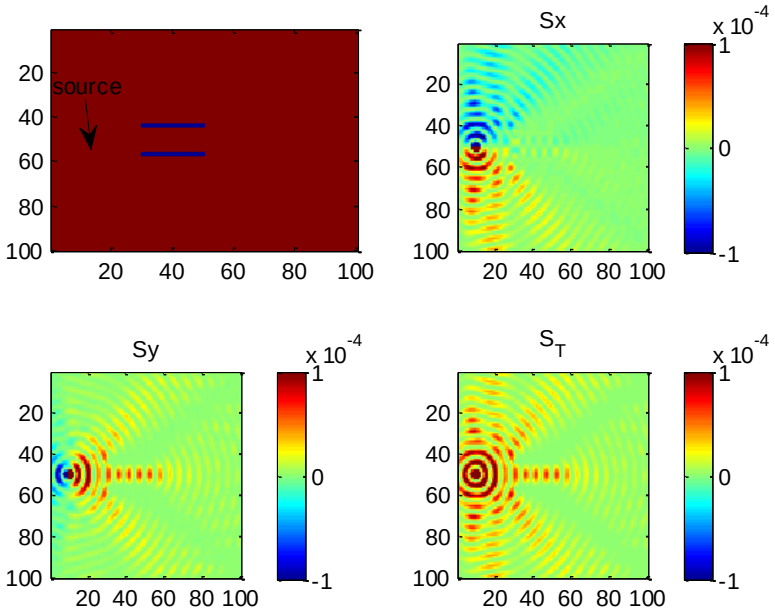

Figure 8. The source of excitation is placed between the left boundary and two parallel strips. The wave is concentrated to propagate between two strips in 2-D.

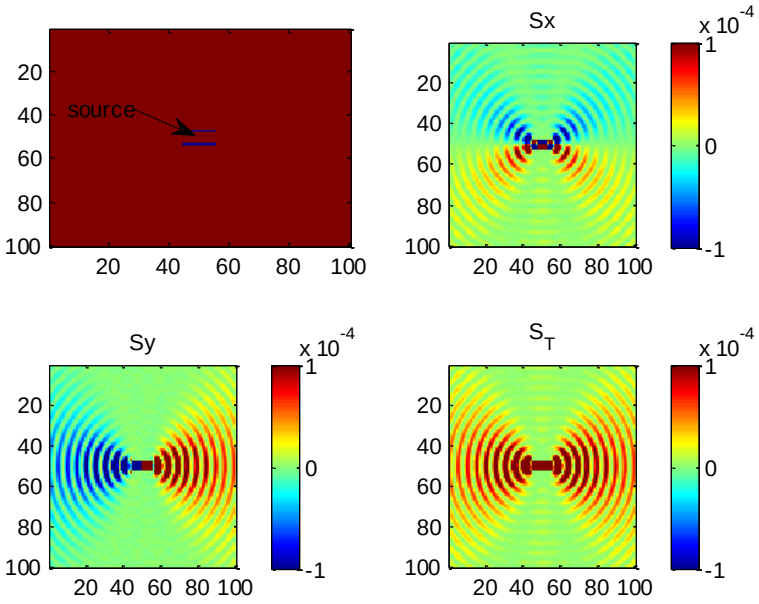

Figure 9. the source is placed between two parallel strips at the centre of a domain in 2-D FDTD.

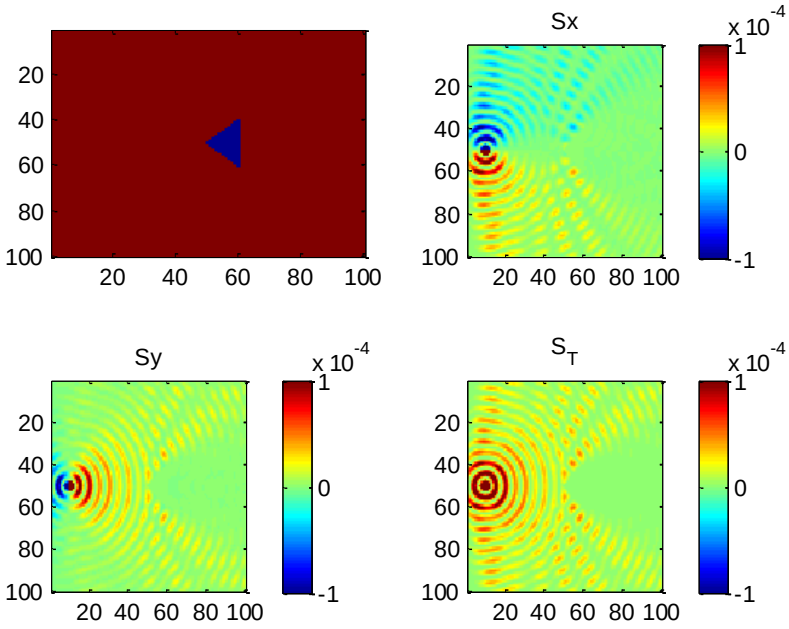

Figure 10. Triangle obstacle shape is placed at the centre of a domain in 2-D.

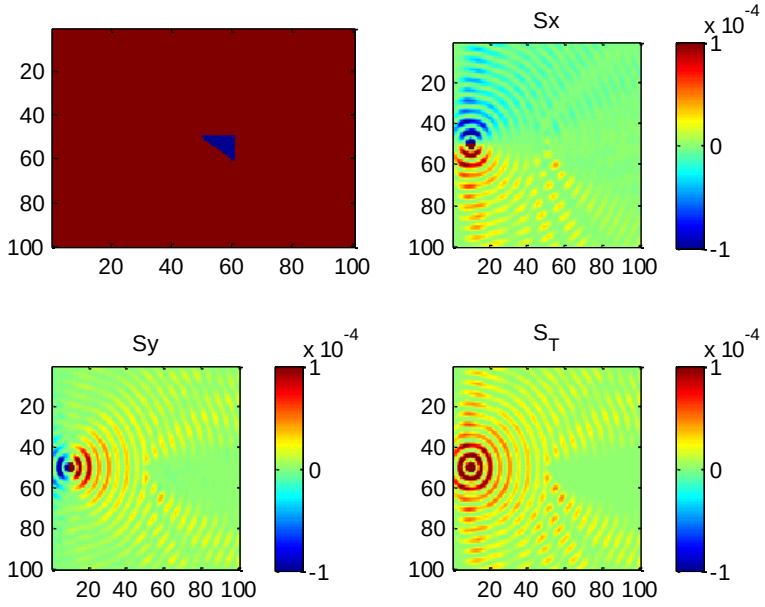

Figure 11. Triangle obstacle shape is placed at the centre of a domain in 2-D.

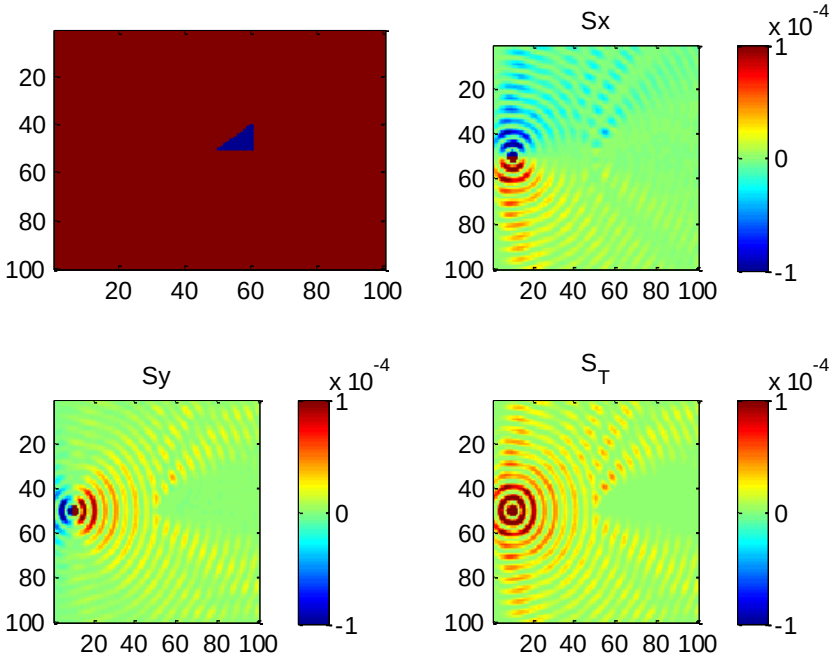

Figure 12. Triangle obstacle shape is placed at the centre of a domain in 2-D.

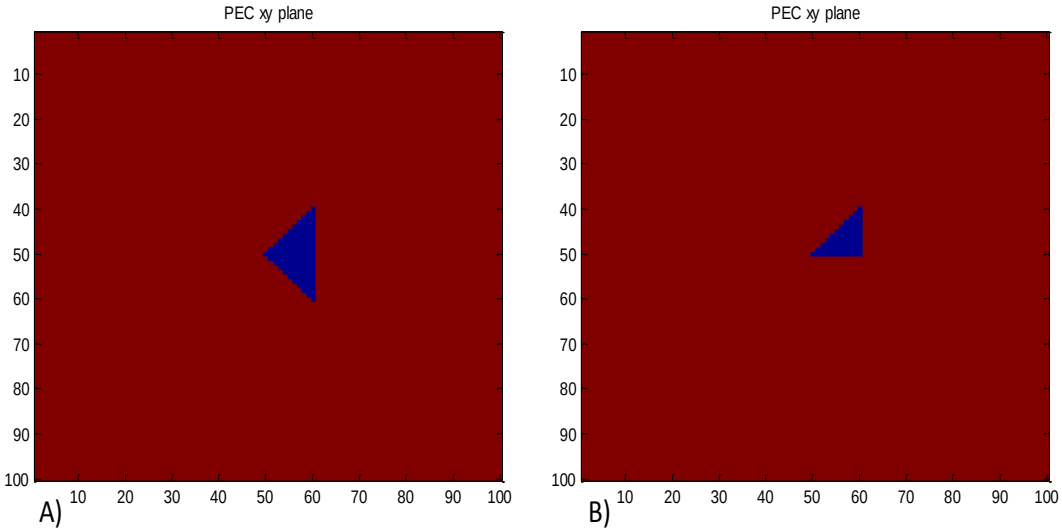

Figure 13. The implementations of two different shapes of obstacles have the electric property of a PEC placed at the centre of a domain. The obstacles constructed in the computational domain as a mesh mode in 3-D FDTD.

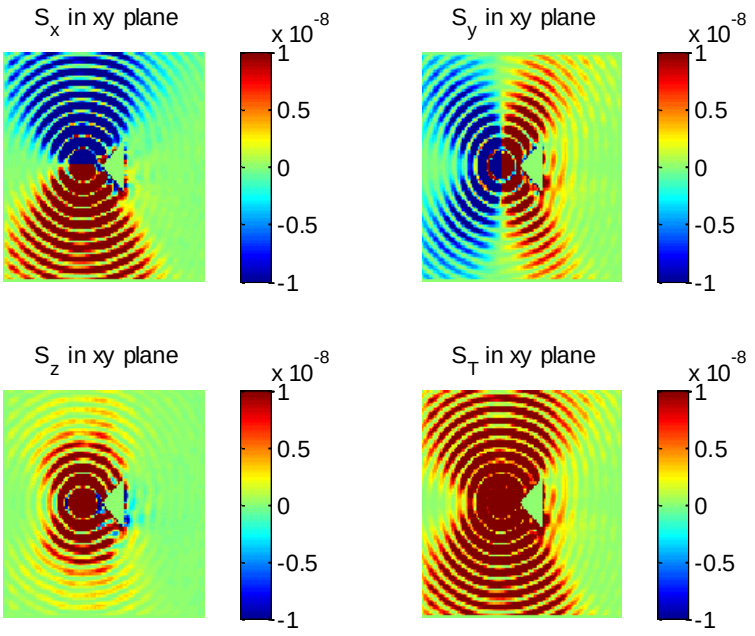

Figure 14. Triangle obstacle shape set as a PEC in domain in 3-D FDTD.

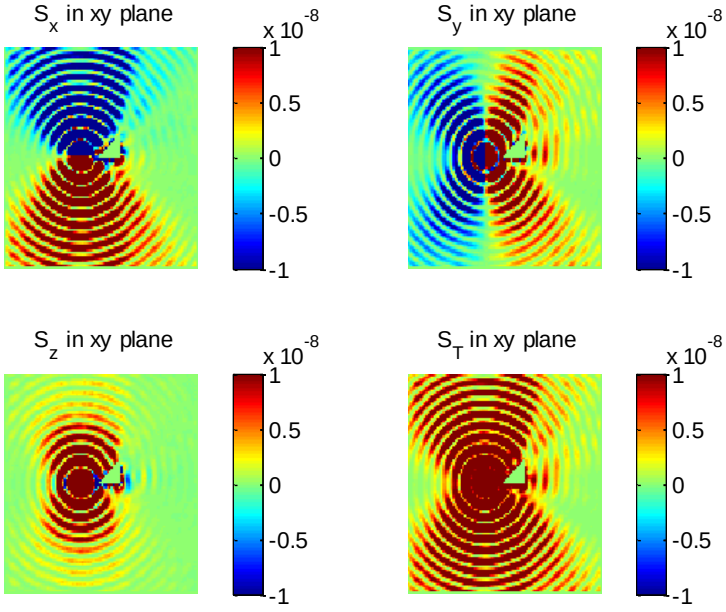

Figure 15. Triangle obstacle shape set as a PEC in domain in 3-D FDTD.

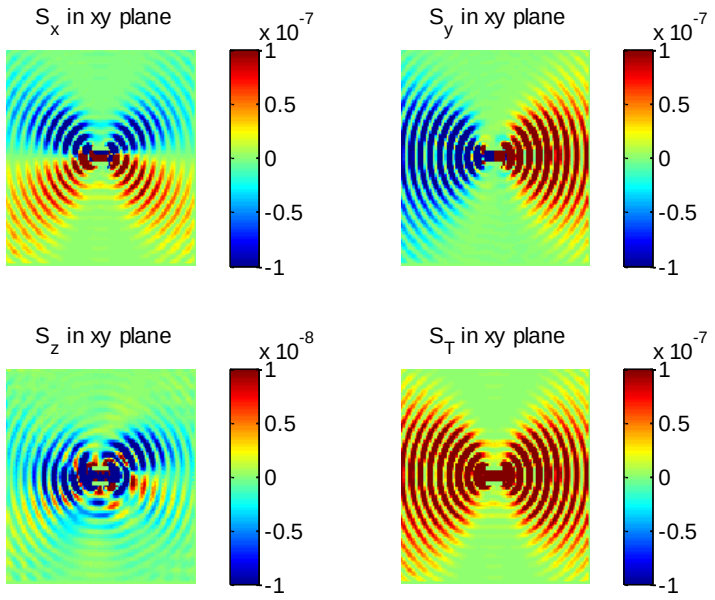

Figure 16: The source of excitation is placed in the middle of two parallel strips in 3-D FDTD domain.

Conclusion

We have demonstrated a solution of the Maxwell's equations by applying the FDTD method. Many different cases have been reported in this work describing the distributions of Poynting vector of EM waves in free space when the EM waves interacted with the obstacles included in a domain. It was found that the FDTD method is extremely useful to apply for solving Maxwell's equations numerically as it is difficult to solve otherwise. The problem analytically as well as the first-order Mur's absorbing boundary condition approach is proved to be an efficient condition to improve the FDTD numerical performance and also saved the computational time.

References

[1] Mur, G. (1981). Absorbing Boundary Conditions for the Finite Difference Approximation of the Time Domain Electromagnetic Field Equations, IEEE Transactions on Electromagnetic Compatibility, EMC-23, 377-382.

[2] Otman, S. and Ouaskit, S. (2017). FDTD simulations of surface Plasmon using the effective permittivity applied to the dispersive media. American journal of electromagnetic and applications, **5**, 14-19.

[3] Khitam, Y. E., Sami, A. A., and Mohammed, M. S. (2018). 3D-FDTD Head Model Exposure to Electromagnetic Cellar Phones Radiation, American journal of electromagnetic and applications, **6**, 42-48.

[4] Tony, W. H., Wang, Y. C. and Li, J. (2016). Development of a 3D staggered FDTD scheme for solving Maxwell's equations in Drude medium, computers and mathematics with application, 71, 1198-1226.

[5] Yee, K. S. (1966). Numerical Solution of Initial Boundary Value Problems Involving Maxwell's Equations in Isotropic Media, IEEE Transactions Antennas and Propagation, 14, 302-307.

[6] Taflove, A. and Morris, E. (1975). Numerical Solution of Steady State Electromagnetic Scattering Problems using the Time Dependent Maxwell's Equations. IEEE Transactions on Microwave Theory and Techniques, **23**, 623-630.